

Rheological evolution of the Mount Meager 2010 debris avalanche, southwestern British Columbia

Gioachino Roberti^{1,3}, Pierre Friele², Benjamin van Wyk de Vries¹, Brent Ward³, John J. Clague³, Luigi Perotti⁴, and Marco Giardino⁴

¹Université Clermont Auvergne, CNRS, IRD, OPGC, Laboratoire Magmas et Volcans, F-63000, Clermont-Ferrand, France

²Cordilleran Geoscience, Squamish, British Columbia V8B 0A5, Canada

³Earth Sciences Department, Simon Fraser University, 8888 University Drive, Burnaby, British Columbia V5A 1S6, Canada

⁴Earth Sciences Department, University of Torino, Via Valperga Caluso 35, 10125 Torino, Italy

ABSTRACT

On 6 August 2010, a large (~50 Mm³) debris avalanche occurred on the flank of Mount Meager in the southern Coast Mountains of British Columbia, Canada. We studied the deposits to infer the morphodynamics of the landslide from initiation to emplacement. Structure from motion (SfM) photogrammetry, based on oblique photos taken with a standard SLR camera during a low helicopter traverse, was used to create high-resolution orthophotos and base maps. Interpretation of the images and maps allowed us to recognize two main rheological phases in the debris avalanche. Just below the source area, in the valley of Capricorn Creek, the landslide separated into two phases, one water-rich and more mobile, and the other water-poor and less mobile. The water-rich phase spread quickly, achieved high superelevation on the valley sides, and left distal scattered deposits. The main water-poor phase moved more slowly, did not superelevate, and formed a thick continuous deposit (up to ~30 m) on the valley floor. The water-poor flow deposit has structural features such as hummocks, brittle-ductile faults, and shear zones. Our study, based on a freshly emplaced deposit, advances understanding of large mass movements by showing that a single landslide can develop multiple rheology phases with different behaviors. Rheological evolution and separation of phases should always be taken into account to provide better risk assessment scenarios.

INTRODUCTION

Landslides are one of the major hazards in mountainous regions. When volcanoes are present in the mountains, the hazard is compounded, as volcanic rocks are weak and hydrothermal alteration further weakens both the volcano and the country rock. Thus, potentially unstable volcanic edifices pose a significant hazard to people living in their vicinity. They are prone to large collapses, which can generate fast-moving debris avalanches that may travel far from their source (Siebert, 2002; van Wyk de Vries and Davies, 2015). Some collapses occur during eruptions, but many happen during quiescent periods and are not directly related to eruptive activity (Friele et al., 2008; Shea and van Wyk de Vries, 2010). Causative factors include rapid uplift and erosion as well as weak materials that form the flanks of the volcanoes and commonly slowly

deform under the influence of gravity (van Wyk de Vries and Francis, 1997; Reid and Brien, 2006; van Wyk de Vries and Davies, 2015).

Volcanic and non-volcanic debris avalanches are complex mass movements in which multiple rheologies can coexist (Iverson et al., 2015; Coe et al., 2016), affecting overall behavior and runout. An understanding of these processes is vital for appropriate modeling, hazard and risk evaluation, and possible mitigation strategies (Kelfoun, 2011; Jakob et al., 2013; Iverson et al., 2015).

The deposits and surface morphology of many prehistoric volcanic debris avalanches have been studied to infer transport and emplacement processes (Vallance and Scott, 1997; Takarada et al., 1999; Capra and Macias, 2000; Bernard et al., 2008; Roverato et al., 2014). Studies of these events, however, are limited, as surface features commonly have been degraded or totally lost. Very few studies document in detail fresh deposits emplaced soon after the events (Plafker and Ericksen, 1978; Glicken, 1996). And even in most of these cases, there is a lack of eyewitness accounts and video documentation.

A landslide in August 2010 at Mount Meager in the southern Coast Mountains of British Columbia (Canada) provided us with a unique opportunity to examine the deposit of a volcanic debris avalanche before it was significantly eroded, and thus to improve understanding of debris avalanche rheology and emplacement mechanisms.

Guthrie et al (2012a, 2012b) provided a first description of the event, including seismic signal analysis, a general geomorphic description, and numerical modeling. Roche et al. (2011) studied the effects of the landslide on the Lillooet River discharge. Allstadt (2013) analyzed the seismic data from the event to infer velocity and emplacement dynamics. Moretti et al. (2015) produced a numerical simulation of the event. At present, there has been no detailed study of the geomorphology and rheology of the 2010 Mount Meager landslide, a gap that we fill in this work.

The objective of this study is to refine understanding of the emplacement kinematics and dynamics and the rheology of the Mount Meager debris avalanche in order to advance knowledge of such events. We achieved this objective by constructing a high-resolution orthophoto and digital elevation model (DEM) using structure from motion (SfM) and through detailed geomorphologic mapping (at 1:1000 scale) and grain-size analysis. This new technology can be applied to other debris avalanches around the world to offer valuable new insights into the morphodynamics of large landslides.

■ SETTING

Mount Meager (2680 m above sea level [asl]) is a Pliocene to Holocene volcanic complex 200 km north-northwest of Vancouver, British Columbia (Fig. 1). It lies within the Lillooet River watershed, 65 km upstream of the town of Pemberton.

The Mount Meager massif is a group of coalescent stratovolcanoes that formed during four episodes of volcanism: one minor Pliocene episode and three major Quaternary episodes. Read (1977, 1979, 1990) subdivided the eruptive products into nine volcanic assemblages. The most recent eruption

was an explosive event that occurred 2350 yr ago (Clague et al., 1995; Hickson et al., 1999). Rocks involved in the 2010 landslide were mainly intrusive porphyritic rhyodacite, flows, and breccia units of the Plinth and Capricorn assemblages—the youngest assemblages in the massif (Read, 1990).

Landslides on Mount Meager

Volcanism, associated hydrothermal alteration, and erosion have weakened the rocks that form the Mount Meager massif, as they have at most stratovolcanoes around the world (Finn et al., 2001; Siebert, 2002; Pola et al., 2014).

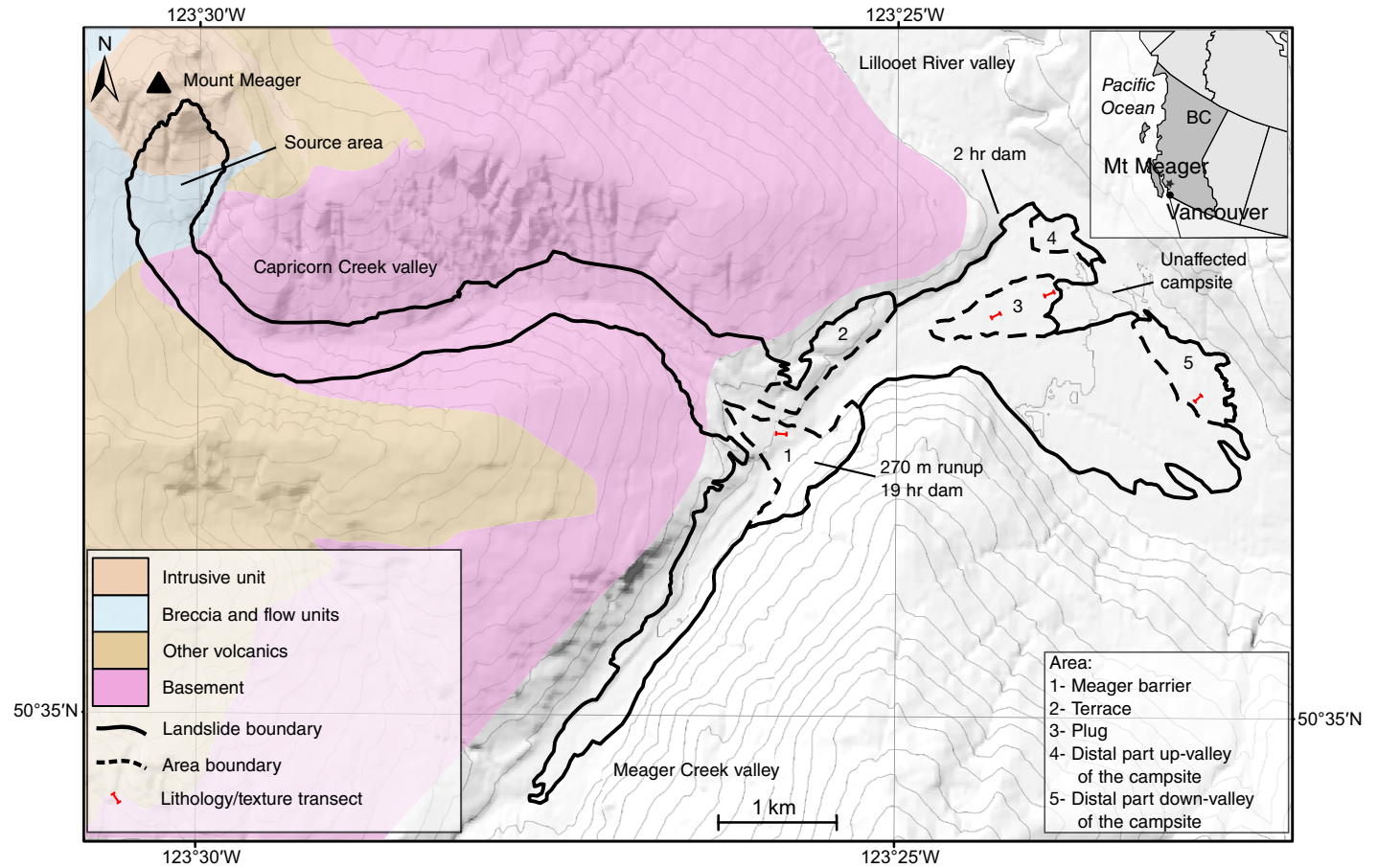


Figure 1. Mount Meager area (British Columbia) (geology after Read, 1979), showing margins of the Mount Meager 2010 landslide, the locations and durations of the landslide dams, and the five deposit areas discussed in the paper. The locations of the lithology transects are shown by red lines. Inset map shows the location of the study area in western Canada (BC—British Columbia).

The considerable topographic relief of the massif (up to 2000 m) and its steep slopes, combined with recent thinning and retreat of alpine glaciers (Holm et al., 2004), have left much of the massif in a state of instability (Read, 1990; Friele et al., 2005; Friele and Clague, 2009).

Evidence of active slope processes affecting the massif include sackungen, debris flows, and debris and rock avalanches (Mokievsky-Zubok, 1977; Jordan, 1994; Bovis and Evans, 1996; Jakob, 1996; Friele and Clague, 2004). In particular, Capricorn Creek, a tributary of Meager Creek, was the source of debris flows and debris avalanches larger than 100,000 m³ in 1931, 1933–1934, 1944–1945, 1972, 1998, 2009, and 2010 (Carter, 1932; Jakob, 1996; Bovis and Jakob, 2000; Guthrie et al., 2012a). Using dendrochronology, Jakob (1996) extended the historical record of landslides in the Meager Creek watershed to 330 yr ago. He identified 13 large debris flows and/or hyperconcentrated flows, an average of one event every 25 yr. These landslides entered Meager Creek and caused significant channel aggradation and instability downstream. Some of them also blocked Meager Creek, forming landslide-dammed lakes (Mokievsky-Zubok, 1977; Bovis and Jakob, 2000; Guthrie et al., 2012a, 2012b). Very large collapses of the flank of the massif have generated at least three Holocene debris flows that traveled downstream to presently populated areas in Lillooet River valley (Friele and Clague, 2004; Friele et al., 2005; Simpson et al., 2006).

The 2010 Event

On 6 August 2010, the south flank and secondary peak (2554 m asl) of Mount Meager collapsed, producing a long-runout debris avalanche (Guthrie et al., 2012a, 2012b) (Fig. 1). The collapse evolved as several subfailures (Allstadt, 2013; Moretti et al., 2015). The debris accelerated to speeds of 60–90 m/s as it traveled 7 km down Capricorn Creek to Meager Creek (Allstadt, 2013). At the Capricorn Creek–Meager Creek confluence, the front of the debris sheet ran 270 m up the opposing valley wall and split into two lobes, one of which ran ~3.4 km upstream and the other 4.7 km downstream to Lillooet River where it spread out over the valley floor before coming to rest 2 km below the Meager Creek–Lillooet River confluence. Field evidence showed that some deposition occurred along the entire travel path, but most of the debris was deposited at the mouth of Capricorn Creek and in Lillooet River valley (Guthrie et al., 2012a, 2012b).

Guthrie et al. (2012a, 2012b) concluded that the 2010 landslide involved the failure of 48.5 × 10⁶ m³ of rock. It thus was similar in size to the 1965 Hope slide in southwest British Columbia (Mathews and McTaggart, 1969; Bruce and Cruden, 1977) and almost twice the size of the famous 1904 Frank slide in southwest Alberta (Cruden and Krahn, 1973; Cruden and Martin, 2007). The vertical elevation drop from the source area to the distal limit of the debris (*H*) is 2185 m, and the total path length (*L*) is 12.7 km. These values yield a fahrboschung (travel angle, $\tan H/L$) of 9.8°. The average velocity of the landslide was 45 m/s (Allstadt, 2013). The landslide produced the equivalent of a M 2.6 local earthquake, with long-period seismic waves that were recorded by seismometers as far away as southern California and northern Alaska.

A mass of debris up to 30 m thick blocked Meager Creek at the mouth of Capricorn Creek, and a 10–15-m-thick debris barrier formed across Lillooet River. A stream gauge on Lillooet River 65 km downstream of Meager Creek recorded an initial rapid drop in discharge, followed ~2 hr later by a rise in discharge after Lillooet River breached its dam. About 19 hr later, discharge spiked following overtopping and breaching of the Meager Creek barrier (Roche et al., 2011; Guthrie et al., 2012a, 2012b). Because this flood wave was built on a low base flow, it did not exceed the bankfull discharge of Lillooet River in Pemberton and caused no property damage.

The outburst floods resulting from the two dam breaches modified much of the original surface of the landslide deposit. However, an extensive area retained its original structure and morphology a year after the event, allowing us to conduct this study.

We use the term “debris avalanche” to describe the 2010 landslide because most of the deposit shows features typical of a volcanic debris avalanche (Glicken, 1991; Ui et al., 2000; Shea and van Wyk de Vries, 2008; Paguican et al., 2014; van Wyk de Vries and Delcamp, 2015). However, the landslide started as a rockslide before rapidly transforming into a channelized debris avalanche. It left a broad range of deposits, which we describe in detail below. They include hummocky faulted debris avalanche deposits, smoother ridges and striated debris flow-like deposits, and deposits from turbid water that scoured bark from trees and embedded stones in trunks.

METHODS

Photography and Structure from Motion

To produce a base map for geomorphic mapping, we took oblique digital photos one year after the landslide with a single lens reflex (SLR) camera during low-level helicopter flights over the accumulation zone. The photos were processed using the SfM and multiview stereo (MVS) algorithms (Snively et al., 2008; James and Robson, 2012; Westoby et al., 2012; Fonstad et al., 2013; Micheletti et al., 2015) to produce three-dimensional topographic models from which we extracted a high-resolution orthophoto (0.08 m/pixel ground resolution) and a DEM (0.34 m/pixel ground resolution). Centimeter-size clasts are resolvable on the imagery.

Uncertainties and limitations of SfM mostly stem from the automated workflow, in which sources of errors are difficult to individualize and control (James and Robson, 2012; Fonstad et al., 2013; Remondino et al., 2014; Micheletti et al., 2015). Nevertheless, the SfM-derived DEMs are comparable in quality to most lidar DEMs (James and Robson, 2012; Westoby et al., 2012; Fonstad et al., 2013; Remondino et al., 2014; Micheletti et al., 2015; Smith et al., 2015).

We also used oblique digital photos taken from a helicopter the morning after the landslide, before the flood from the Meager Creek dam breach. Although these photos could not be used for SfM analysis, they were useful for evaluating geometries and facies relations that were subsequently destroyed by the flood.

Field Mapping

We produced a geomorphic map of the landslide deposits at a scale of 1:1000 from field observations made between August and October 2012 and from the orthophoto and the DEM. We identified and classified geomorphic features, facies, and related facies associations within those parts of the deposit that had not been modified by erosion. For the purpose of discussion, we subdivide the debris avalanche deposit below the mouth of Capricorn Creek into five areas that we refer to as Meager barrier, terrace, plug, distal up, and distal down (Figs. 1 and 2).

Creek into five areas that we refer to as Meager barrier, terrace, plug, distal up, and distal down (Figs. 1 and 2).

Grain-Size and Lithologic Analysis

We chose four sample sites distributed along the length of the deposit from the Meager barrier to the distal margin for grain-size and lithological analyses (Fig. 1). At each site, we placed a 100 m tape parallel to the flow direction. Clast

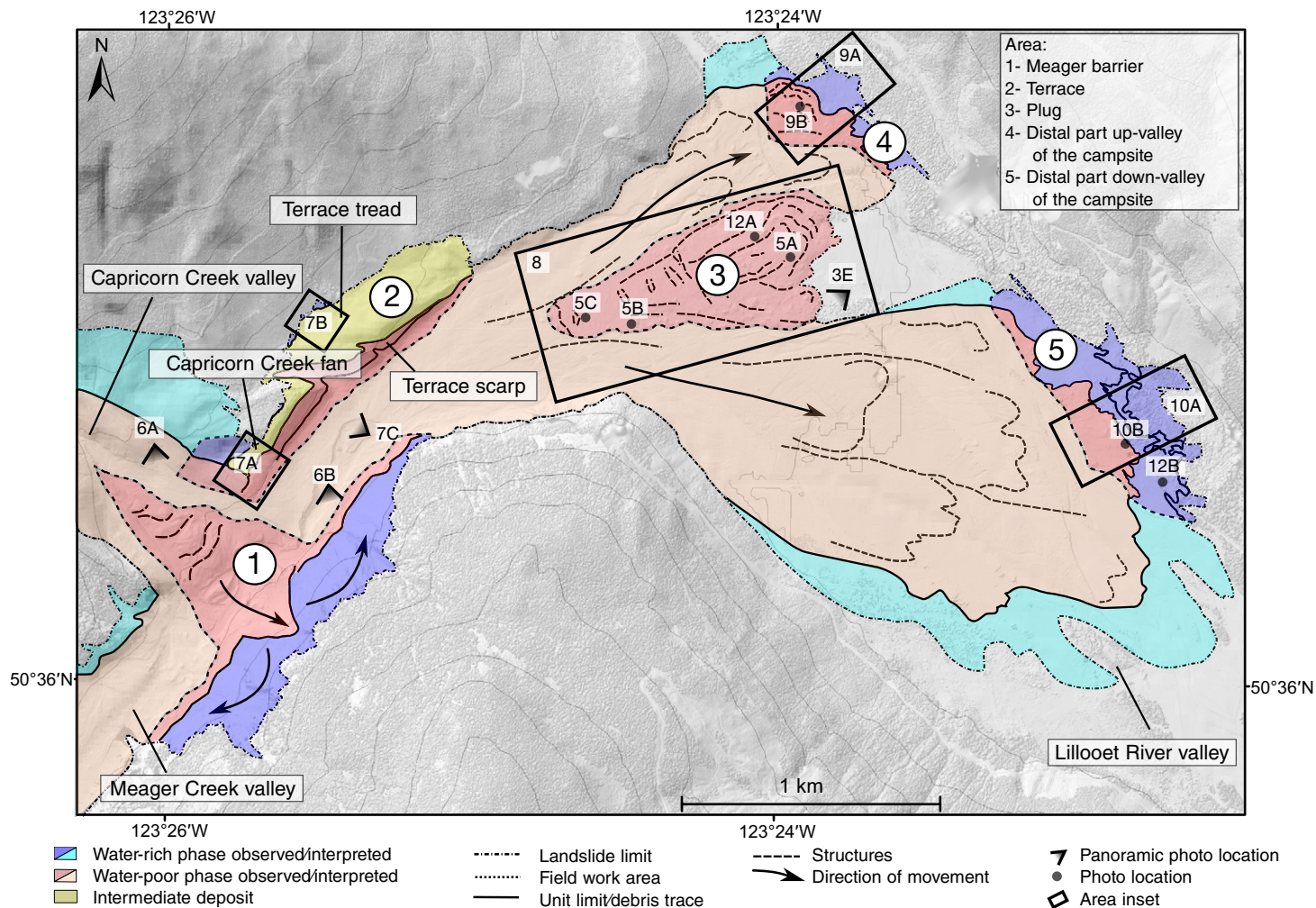
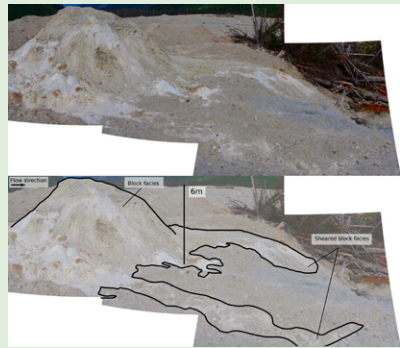
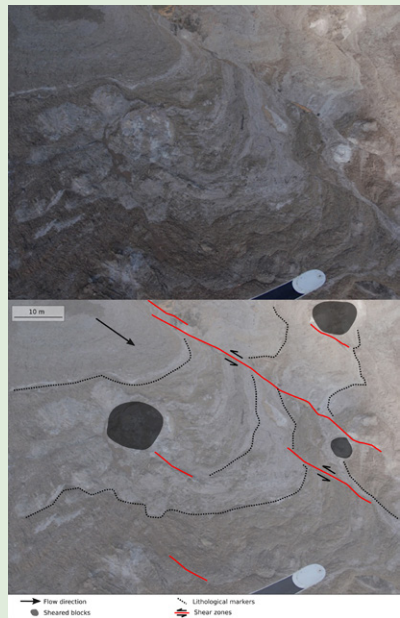


Figure 2. Map of Mount Meager landslide deposits and structures. Also indicated are locations of photographs shown in other figures. Numbers in circles identify the five deposit areas.



¹Supplemental File 1. Photo of a block forming a hummock with related streaks of sheared block facies in area 3. Please visit <http://doi.org/10.1130/GES01389.S1> or the full-text article on www.gsapubs.org to view Supplemental File 1.



²Supplemental File 2. Helicopter view of the debris avalanche surface before the dam breach. Shearing and lithological markers are evident. Please visit <http://doi.org/10.1130/GES01389.S2> or the full-text article on www.gsapubs.org to view Supplemental File 2.

lithologies were recorded at 1 m intervals along the tape and visually classified as basement rock (B), gray porphyritic felsic rhyodacite (GPF), red porphyritic felsic rhyodacite (RPF), and other volcanic rocks (OV). “Other volcanic rocks” include gray, red, and white aphanitic rocks, gray and cream colored porphyritic rocks, and pumice. One-kilogram bulk samples were collected for grain-size analysis at stations 20, 40, 60, 80, and 100 m along the tape. For each of these samples, 100 of the largest clasts >4 mm retained from sieving were also lithologically classified. Ten other bulk samples were collected from selected stations on the deposit, two from mixed debris and four each from pulverized blocks and altered blocks.

The samples were split into >1 mm and <1 mm fractions. The 1–4 mm fraction was dry sieved while the <1 mm fraction was submitted to ALS Global Laboratory (Burnaby, British Columbia) for hydrometer analysis following ASTM protocol D422. We then integrated the sieve and hydrometer data to produce grain-size distributions truncated at 4 mm.

RESULTS AND DISCUSSION

We first describe facies, structures, and hummocks, and then describe and interpret each of the five areas that constitute the debris avalanche deposit.

Facies

The **block facies** comprises highly brecciated but intact masses of red or gray rhyodacite, altered cream colored rhyodacite, and altered and unaltered basement rock derived from the source area. Blocks are tens to hundreds of cubic meters in volume and form hummocks one to several meters high. They commonly have a “jigsaw puzzle” fabric (Fig. 3A) and a silt-to-clay loam matrix. The fine fraction (<2 mm) of zones of hydrothermally altered blocks contains 19%–29% clay, whereas the fine fraction of unaltered blocks contains 2%–5% clay (Fig. 4).

The **sheared block facies** is localized in shear zones within the block facies and occurs as discrete zones or streaks of coherent lithology in the deposit. It is a product of fragmentation and disaggregation of blocks by shear during the final stage of debris emplacement (Supplemental Files 1¹ and 2²). The form of the block facies has been destroyed, but the lithology of the source block has been retained. Streaks of sheared block facies define the direction of movement of the debris avalanche (Figs. 3C–3E).

The **mixed facies** is a fully mixed debris consisting of brown matrix-supported diamicton (Figs. 3B, 3C, and 3E). It comprises particles ranging from clay to medium-size boulders. The matrix (<2 mm) is a sandy loam, with a clay content of 3%–8% (Fig. 4). The gravel fraction consists of 19%–29% basement rock, 49%–64% gray porphyritic rhyodacite, 4%–10% red porphyritic rhyodacite, and 9%–12% other volcanic rocks. This facies also contains

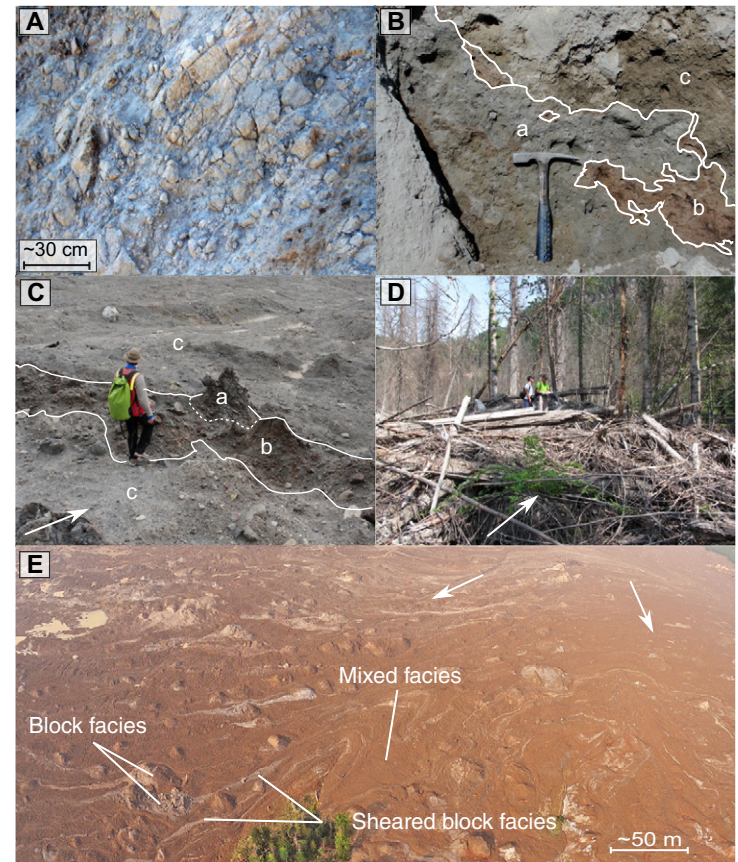


Figure 3. Photographs of typical Mount Meager landslide deposit facies. White arrows indicate flow direction. (A) Block facies. (B) Contacts between mixed facies (a), sheared block facies of gray rhyodacite (b), and sheared block facies of red rhyodacite (c). Hammer is ~30 cm. (C) A coherent but highly brecciated block (a) disaggregated by shear to form sheared block facies (b). The surrounding material is mixed facies (c). (D) Woody debris facies. (E) Aerial photograph of the debris avalanche deposit in Lillooet River valley taken the morning after the event, before the dam on Meager Creek breached (photo courtesy of D.B. Steers).

abraded wood fragments, and its surface supports rare kettle holes left from the melt of blocks of glacier ice derived from Capricorn Glacier in the source area.

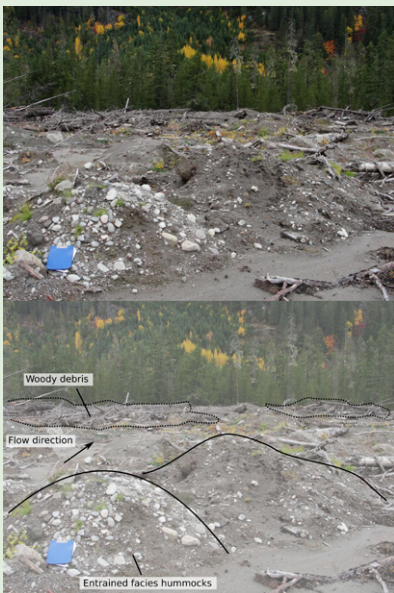
The **woody debris facies** comprises partially abraded tree stumps, stems, and branches derived from the forest destroyed by the debris avalanche and pushed to the margins of the deposit (Fig. 3D).



³Supplemental File 3. Photo of an outcrop showing relations among facies in area 1. Please visit <http://doi.org/10.1130/GES01389.S3> or the full-text article on www.gsapubs.org to view the Supplemental File 3.

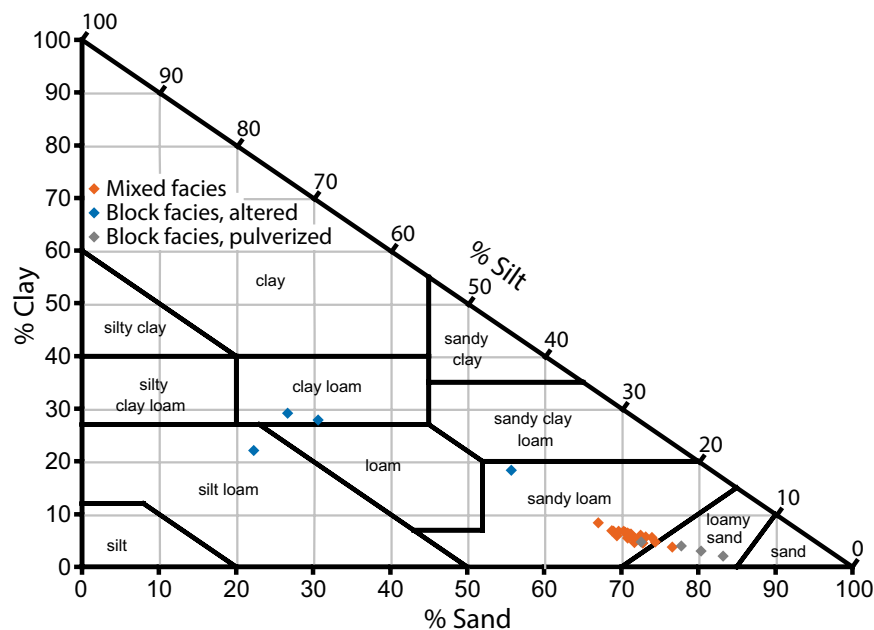


⁴Supplemental File 4. Photo of an outcrop section through a hummock showing facies relations in area 3. Please visit <http://doi.org/10.1130/GES01389.S4> or the full-text article on www.gsapubs.org to view Supplemental File 4.



⁵Supplemental File 5. Photo of entrained-facies hummocks in the water-rich phase of the deposit, area 4. Please visit <http://doi.org/10.1130/GES01389.S5> or the full-text article on www.gsapubs.org to view Supplemental File 5.

Figure 4. Sand-silt-clay ratios of samples of the Mount Meager debris avalanche matrix. Fields indicate the 12 classes of soil textural classification (Soil Survey Division Staff, 1993).



The **entrained facies** consists of fluvial channel or overbank sediments and colluvium incorporated into the landslide by scour and thrusting. This facies is distinguished from others by its well-sorted texture and rounded and sub-rounded clasts. The entrained facies is a minor constituent of the landslide deposit (Supplemental File 3³).

Structures

The principal structures are linear forms associated with thrust, normal, and strike-slip faults. They include scarps, ridges, and linear depressions and, in some cases, mark lithological and facies boundaries (Fig. 5).

Compressional ridges are perpendicular to flow. They are rounded and commonly sinuous along their length (Fig. 5A). At eroded edges of the deposit, compressional ridges are underlain by diffuse shear zones or thrust faults marked by displaced lithologies.

Strike-slip faults are meter- to multi-meter-wide linear depressions with low relief, oriented parallel to the flow direction (Fig. 5B). They are commonly associated with splay faults, grabens, and compressional ridges.

Normal faults are marked by scarps with straight slopes (Fig. 5C). In some cases, they occur in pairs and form grabens (Fig. 5D). Normal faults strike perpendicular to the flow. Where seen in cross-section, normal faults are either single sharp faults or broad shear zones (Fig. 5D).

Hummocks

Hummocks are 1–8 m in height, 1–40 m in length, and 1–30 m in width; volumes range from 1 m³ to ~2 × 10³ m³. Shapes are round or ellipsoidal. Hummocks are composed of block facies (either gray or red porphyritic rhyodacite), entrained facies, or a mix of block, mixed, and sheared block facies.

Mixed hummocks typically have a core of block facies and sheared block facies and a carapace of mixed facies (Supplemental File 4⁴). The boundary between the core and carapace is sharp to gradational; in some cases flame structures intrude the core.

The entrained facies hummocks are composed of either fluvial sand and gravel or sand (Supplemental File 5⁵). This hummock type is rare and found only at the distal margin of the debris avalanche. The entrained facies hummocks are smaller than the block and mixed hummocks, with a volume of ~1–3 m³.

Area Descriptions

Area 1: Meager Barrier

The southeastern valley wall of Meager Creek, opposite the mouth of Capricorn Creek (area 1 in Figs. 1 and 2), was stripped of all trees up to 270 m above the valley floor by the landslide. Only a patchy veneer of landslide debris

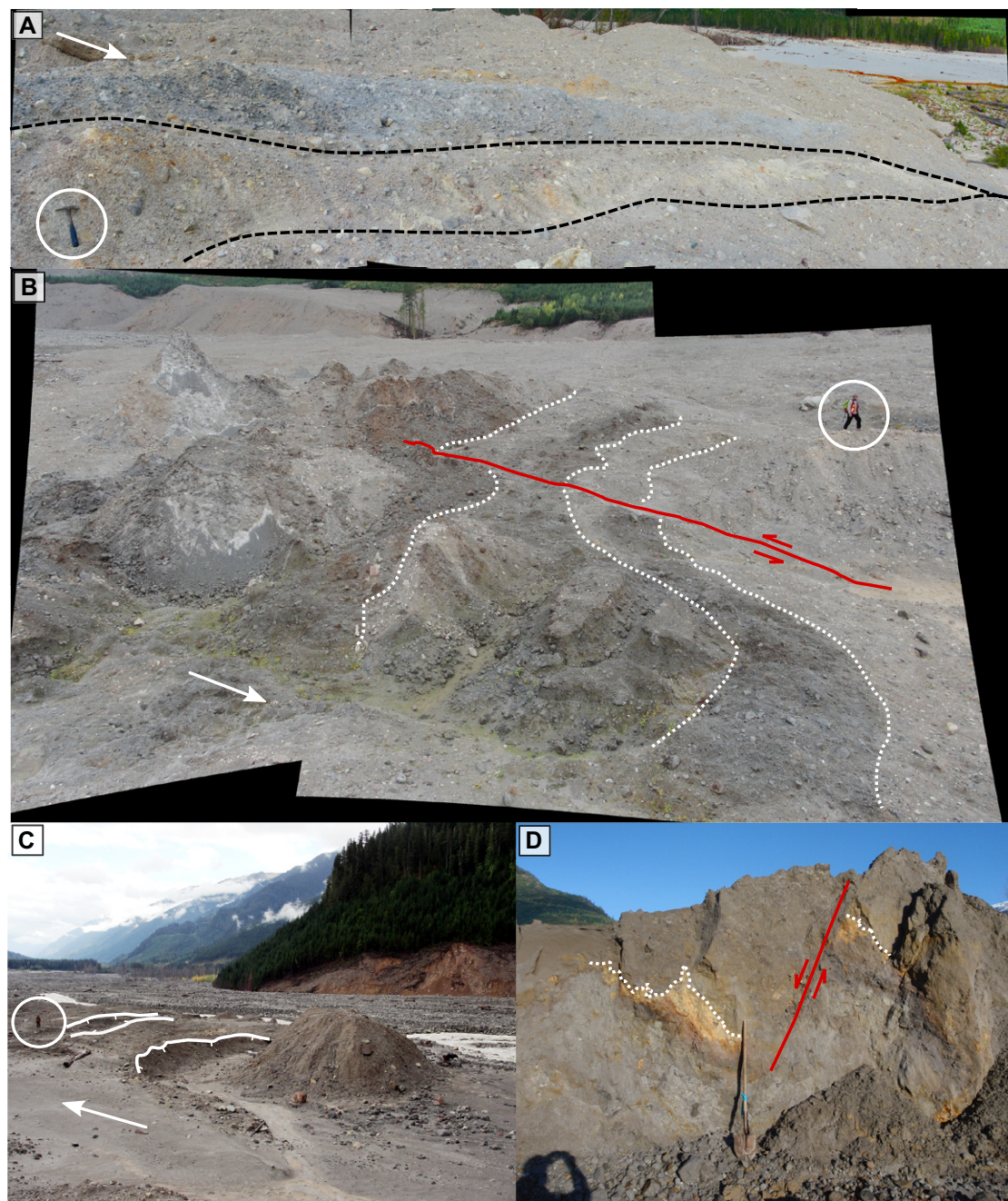


Figure 5. Photographs of typical structures in the Mount Meager landslide debris. White arrows indicate flow direction. (A) Compressional ridges (hammer ~30 cm). The black lines show thrusts separating compressional ridges of gray rhyodacite and cream-colored, altered sheared block facies. (B) Panoramic view of a shear zone (circled person for scale). The red line marks a strike-slip fault; the white dotted lines highlight lithological markers that show the displacement along the fault. A graben is visible in the foreground. (C) View down Lillooet River valley showing extensional features in the plug; normal fault scarps are indicated by white lines. The graben in front of the circled standing person is perpendicular to the flow direction. Note the runup on the valley side. (D) Normal fault trace exposed in section. White dotted lines here indicate lithological markers. The shovel is 1.5 m in length.



⁶Supplemental File 6. Helicopter view of the Meager barrier before the dam breach. Photo courtesy of D.B. Steers. Please visit <http://doi.org/10.1130/GES01389.S6> or the full-text article on www.gsapubs.org to view Supplemental File 6.



⁷Supplemental File 7. Helicopter view of the Meager barrier after the dam breach. Photo courtesy of D.B. Steers. Please visit <http://doi.org/10.1130/GES01389.S7> or the full-text article on www.gsapubs.org to view Supplemental File 7.

remains on this slope. At the foot of the slope, and extending across Meager Creek valley to the mouth of Capricorn Creek valley, is thick debris forming the barrier that dammed Meager Creek for 19 hr. The Meager barrier deposit is 700 m long, 50–500 m wide (increasing in width from the apex to the southeastern side of the valley), and ~30 m thick, thinning toward Capricorn Creek.

The barrier supports irregular ridges that are perpendicular to the flow direction (Fig. 6A). Seven major compressional ridges are present on the northwestern side of the barrier. In contrast, the southernmost 200 m of the barrier surface, nearest the southeastern valley wall, is an irregular hummocky deposit.

The compressional ridges are southeast verging and identified by a basal thrust. The difference in height between each depression and the tops of adjacent ridges is as much as 12 m. The ridges increase in length from 50 to 300 m in a northwest-southeast direction; the longest ridges span the full width of

the deposit. Streaks of sheared block facies trend parallel to the ridges (Supplemental File 6⁶). Only a few blocks, in the form of low broad hummocks, rise above the surface of the Meager barrier. Larger blocks (up to 900 m³) locally underlie the ridges (Supplemental File 7⁷). We observed only a few altered blocks in this area.

The 200-m-long distal portion of the Meager barrier, below the opposing wall of Meager Creek, was eroded during the dam breach, but pre-breach helicopter photos (Fig. 6A) show a northwest-verging thrust associated with a ridge, indicative of compression and contraction. Many hummocks of gray rhyodacite are present near the valley side in this area.

Three lineaments are evident on the southeastern valley wall above the barrier (Fig. 6B). The highest lineament is a debris line that extends up to 270 m above the valley floor and marks the limit of the debris avalanche on the slope. The debris boundary separates the area stripped of trees from un-

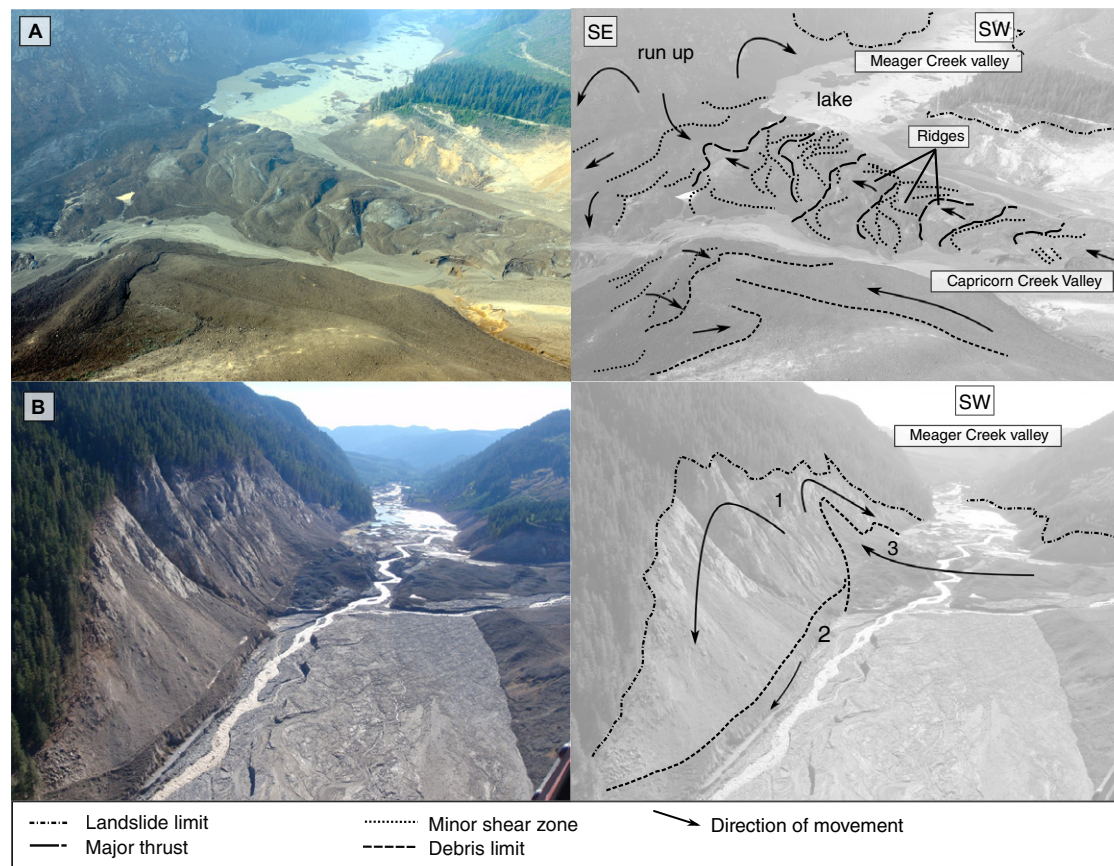


Figure 6. (A) Sketch of the Meager barrier (area 1) based on a photograph taken before the dam breach, showing compression. (B) Sketch of the barrier area after the dam breach. The limit of the debris avalanche and lower debris lines on the valley side are marked: 1—high lineament caused by runup of the first pulse; 2—debris line left by the bulk of the mass flowing toward Lillooet River valley; 3—debris line left by runup and collapse of Meager barrier debris. Arrows indicate the direction of movement. Photos courtesy of D.B. Steers.

disturbed forest. An intermediate lineament marks the limit of the debris barrier on the slope. The lowermost lineament is ~20 m above the valley floor and is consistently parallel to it.

Area 1: Interpretation

The front of the debris avalanche swept across Meager Creek and ran up the southeastern wall of the valley, completely removing the forest and scouring the forest floor. The maximum limit reached by the debris is marked by the conspicuous trimline high on the valley wall. In the barrier deposit, the major compressional ridges formed at the foot of the slope as the forward movement of the debris avalanche in this area was impeded and the debris was compressed. The debris stopped first at its front while the back was still moving. We interpret the Meager barrier deposit to be related to seismometer “signal H” of Guthrie et al. (2012a) and the “aftershock” of Allstadt (2013), representing a final summit collapse of the secondary Mount Meager peak ~2 min after the main event. The hummocks of gray rhyodacite at the foot of the opposing slope are likely a product of runup and collapse of this late-stage emplacement.

We interpret the three lineaments on the southeastern valley wall to have formed during different phases of the debris avalanche. The high lineament was produced by the energetic and mobile front of the water-rich phase of the debris avalanche. The intermediate line is slightly younger and associated with barrier emplacement (Fig. 6B). The lowest line marks the trace of the valley-confined flowing mass—the water-poor phase—that reached Lillooet River valley.

Area 2: Terrace

The terrace (area 2 in Figs. 1 and 2) is located on the northwestern side of Meager Creek. It lies ~60–100 m above the valley floor and is underlain by glacial sediments. Remnants of two Holocene fans overlie the terrace at the mouth of Capricorn Creek. Both of the fans, and the terrace itself, were incised by Capricorn Creek sometime during the Holocene. The modern pre-2010 Capricorn Creek fan is inset into the terrace. Part of the frontal wave of the debris avalanche ran up onto the terrace northeast of Capricorn Creek after being deflected off of the valley wall in area 1. It removed second-growth forest on the terrace and left a veneer of debris. We recognize three subareas of area 2: (1) the Capricorn Creek fan, (2) the terrace tread, and (3) the terrace scarp.

The Capricorn Creek fan subarea is characterized by two fan levels, both of which are inset into the terrace. The lower fan surface is 20 m above the floor of Capricorn Creek and extends ~250 m up Capricorn Creek and 160 m down Meager Creek. The higher fan surface is 60 m above the floor of Capricorn Creek and extends 200 m down Meager Creek. Two units, *a* and *b*, of landslide debris are present within the Capricorn Creek fan (Fig. 7A). Unit *a* occurs in what Guthrie et al. (2012a) termed “the spray zone”, a discontinuous veneer of silt, sand, and gravel within an area of stripped and damaged trees at the limit

of the debris avalanche. Unit *b*, which borders unit *a*, is a blanket of mixed-facies material with a surface characterized by up to 1-m-high compressional ridges and longitudinal and transverse ridges. Unit *b* has three lobes; the first, *b1*, is a major northwest-southeast-trending debris ridge parallel to the terrace scarp on the northeastern side of Capricorn Creek. It is 220 m long, 25 m wide, and 2 m high. The second lobe, *b2*, is associated with an east-west-oriented fold that is 70 m wide and 100 m long. This lobe contains an east-west ridge that is 10 m wide, 80 m long, and 0.5 m high. A third debris lobe, *b3*, overlaps lobes *b1* and *b2* and is parallel to and near the edge of the terrace.

The second subarea of area 2—the terrace tread—extends ~600 m along Meager Creek valley. It is up to 200 m wide and 60–80 m above the valley floor. The tread is dissected by five gullies that are older than the landslide (Fig. 2). Two units of landslide debris (*a* and *b*), similar to those present in the Capricorn Creek fan, are present here (Fig. 7B). Unit *a*, located between the undamaged forest and unit *b*, comprises a thin layer of discontinuous debris within a zone of stripped and damaged vegetation up to 30 m wide. Downed tree stems at the margin of the deposit indicate the direction of flow, which is slightly transverse to the trend of the limit of the landslide. Lobes of debris entered the forest obliquely to the main flow direction. Unit *b* sharply borders unit *a* along a front 0.5–1 m high and comprises scattered block facies hummocks within a blanket of mixed facies up to 1.5 m thick. Compressional ridges 10–20 m long, 1–8 m wide, and up to 0.5 m high are parallel to the valley side. The hummocks are up to 12 m in diameter and 2.5 m high. Some of the hummocks have extensional grabens and partially collapsed sides. The boundary between units *a* and *b* at the downstream end of the terrace coincides with a concentration of altered blocks and sheared block facies streaks.

A thin veneer of mixed-facies debris covers the third subarea of area 2—the terrace scarp. Two lineaments are present on the scarp and are parallel to its margin (Fig. 7C). The higher lineament, which is about one-third of the vertical distance below the top of the terrace, slopes down-valley and merges with the valley floor at the end of the terrace. It is continuous with lobe *b3* in the Capricorn fan area and extends up the largest upstream gully dissecting the terrace. The lower lineament is ~5 m above the valley floor. The two lineaments merge at the down-valley end of the scarp.

Area 2: Interpretation

The many units and debris lines present in this area indicate that the terrace records different landslide pulses. In the terrace fan, unit *a* and lobe *b1* are traces of the flow coming down Capricorn Creek before reaching the Meager Creek valley side. Unit *a* is the deposit of the frontal highly mobile flow (water-rich phase), while *b1* is of the less-mobile debris-rich flow (water-poor phase). Lobes *b2* and *b3* are the deposits of different pulses of the flow after the impact on the southeastern wall of Meager Creek valley. Then the debris avalanche overrode the terrace tread and scarp. On the terrace tread, unit *a* is the expression of the frontal water-rich phase, and unit *b* is the deposit of an intermediate-water-content phase. Unit *b* on the terrace tread was water-rich

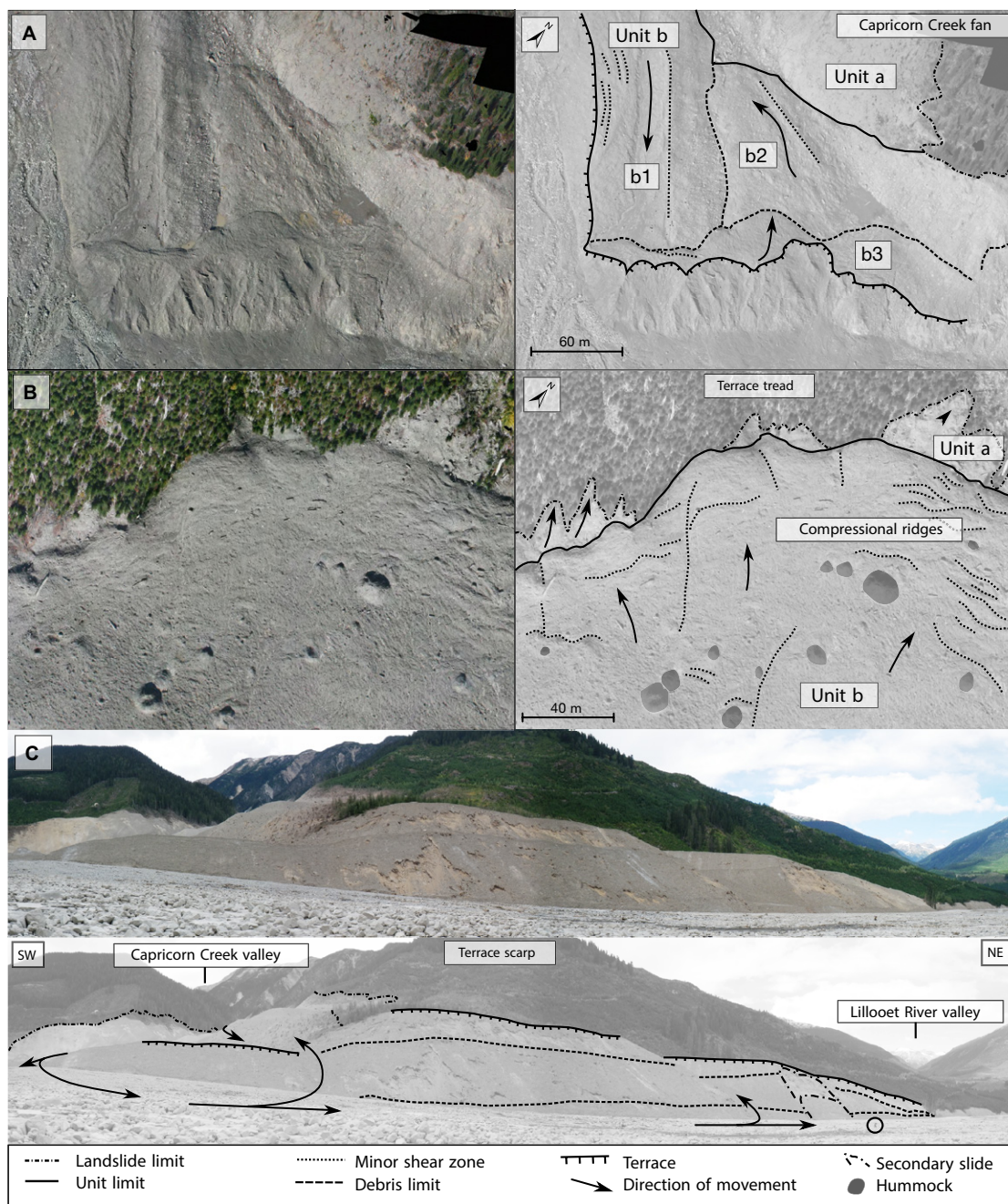


Figure 7. (A) Orthophoto of the Capricorn Creek fan (part of area 2 of the Mount Meager landslide), showing unit *a* and unit *b* (the latter a product of three lobes: *b1*, *b2*, and *b3*). (B) Orthophoto of the central portion of the terrace tread showing unit *a* (water-rich flow deposit) and unit *b* (intermediate-water-content phase). The latter supports hummocks and deformation structures. Ridges indicate compressional motion against the valley side. (C) Panoramic view of the terrace scarp, debris trimlines, and post-depositional sloughing (person in the circle at lower right for scale). Image courtesy of C.-A. Lau.

enough to run over the terrace but could still support structures and hummocks. It is continuous with *b2* on the terrace fan. The debris lines on the terrace scarp correlate with pulses of the water-poor phase. The upper debris line is continuous with lobe *b3* and marks the maximum thickness of the water-poor material responsible for the plug deposit (see below); the lower line records the tail of the flow, or a surge related to the final “aftershock” collapse at the headwall of the landslide.

Area 3: Plug

The plug is in the center of the Meager Creek fan in Lillooet River valley (area 3 in Figs. 1 and 2). It has a triangular shape and is ~1200 m long and 100–500 m wide. Debris of the 2010 landslide in this area is up to 15 m thick. Lateral lobe wings and late-stage slurries were present along the external margins of the lobes but were removed by the dam-breach flood.

The plug is composed of block, sheared block, and mixed facies, with lithologic zoning resulting from the disaggregation of blocks into long tails, streaks, and discrete zones of sheared block facies. Hummocks are common and are 1–8 m high, 1–30 m wide, and 1–40 m long; they have volumes of $1\text{--}2 \times 10^3 \text{ m}^3$. Low areas between hummocks exhibit deformation structures including shear zones, ridges, grabens, and lobes.

The west end of the plug, where Meager Creek enters Lillooet River valley, is characterized by collapsed hummocks, thrust and strike-slip faults, and well-developed grabens. Compressional features are cut by shear structures that are, in turn, cut by extensional structures (Fig. 8).

Farther east, toward the center of the plug area, the deposit is characterized by flow-parallel strike-slip faults. The faults are dextral and oriented southwest-northeast on the north side of the plug, and sinistral and oriented west-east on the south side. Grabens transverse to the flow direction have northwest-southeast orientations (Fig. 8). Strike-slip faults occur in areas of ridges, depressions, and sheared hummocks and mark the boundaries between the central part and the lateral parts of the debris avalanche that continued to flow to the east.

Two distal debris lobes extend from the main mass of debris and terminate on the Lillooet River floodplain with sharp fronts 7–10 m high, forming the east edge (front) of the plug. The point where the two lobes separate is 620 m from the west end of the plug. The more northerly lobe is 500 m long and up to 330 m wide. The southerly lobe is 450 m long and up to 150 m wide. The northern lobe is characterized by an echelon sigmoidal ridges, bounded by shear zones that accommodated the deformation at the point of bifurcation. The distal front of the lobe is marked by compressional ridges oriented northwest-southeast and northeast-southwest that terminate against and partially overtop hummocks. The north margin of the lobe is characterized by a system of dextral strike-slip faults spaced 30–50 m apart and oriented southwest-northeast. They displace hummocks and form pull-apart basins and push-up landforms. The strike-slip faults separate steps and drop down to the north-northwest.

In the southern lobe, the flow direction changes from southeast to east, then to the northeast. Strike-slip faults on the north side of this lobe are sinistral; those on the south side are dextral (Fig. 8). The area between the two lobes has an irregular surface morphology, which we attribute to compression and thrusting by the debris flowing around it; some dead trees are still standing in this area.

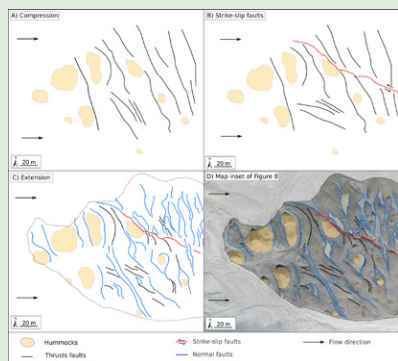
In photos taken the morning after the landslide (Fig. 3E) and before the breach of the Meager barrier, fluid slurries are visible at the margins of the plug. Muddy afterflow continued from Capricorn Creek valley for days after the event as loose debris was eroded and flushed downstream by the creek.

Area 3: Interpretation

The hummocks are rigid portions of the landslide mass that commonly slowed and came to rest sooner than the surrounding material. This is evidenced by flow structures and spreading and extension of some hummocks in the flow direction. As the hummocks were carried, rotated, and tilted by the flowing mass, they were also deformed, fractured, and disaggregated. Mixed material wraps around individual hummocks.

Discrete faults, shear zones, pull-apart basins, and push-up structures are evidence of the dynamic interactions between different parts of the flowing mass. Cross-cutting relations between faults indicate multiple generations of deformation structures. Differential movement of the debris led to localized compressional, extensional, and transtensional stresses. Extensional structures are dominant at the west end of the plug, where they cut thrust and strike-slip faults. Strike-slip structures are dominant in the central part of the plug, cutting and displacing thrusts. Later normal faults are also present in this area, providing evidence for a change from a compressional to an extensional regime. The plug front to the east is dominated by thrust faults, reflecting the compressional regime in the area. There is no evidence of a highly mobile water-rich phase extending beyond the steep leading east edge. This may be related to different trajectories of the frontal wet-phase and the subsequent dry-phase flows. The water-rich phase had higher mobility and caromed more as it traveled down Meager Creek. The water-poor phase had lower mobility and stayed more valley confined.

Geometrical patterns and kinematic indicators allow a possible reconstruction of the deformation history of the debris in the plug area (Supplemental File 8⁸). Primarily, compression dominated as debris, flowing in a single direction, rapidly decelerated at the flow front. Then, the debris started to flow in several different directions while decelerating at different rates. Lateral margins of the plug continued to move and deposit debris downstream in areas 4 and 5. Strike-slip faults formed to accommodate the deformation. Finally, the debris mass stopped and there was a general spreading and relaxation, with normal faults forming over the entire surface. The later slurries indicate that after the emplacement of the plug material, water remobilized part of the debris.



⁸Supplemental File 8. Sketch showing the inferred structural evolution of the west end of the plug. (A) First compressional ridges formed as the front started to decelerate. (B) The debris divided into different lobes, and strike-slip faults accommodated the differential motion. (C) This area stopped while the front was still moving. Normal faults accommodated the consequent extension. (D) Inset map of the west end of the plug. Extensional structures dominate this area. Please visit <http://doi.org/10.1130/GES01389.S8> or the full-text article on www.gsapubs.org to view Supplemental File 8.